JOURNAL OF CATALYSIS 125, 292–310 (1990)

Structure and Catalytic Properties of Silica-Supported Polyoxomolybdates

I. Mo/SiO_2 Catalysts Prepared from Hexamolybdate

CLAUDE ROCCHICCIOLI-DELTCHEFF,* MOHAMED AMIROUCHE,* MICHEL CHE,† JEAN-MICHEL TATIBOUËT,† AND MICHEL FOURNIER,*

Laboratoire de Physicochimie Inorganique (URA 419-CNRS) and †Laboratoire de Réactivité de Surface et Structure (URA 1106-CNRS), Université Pierre et Marie Curie, 4 place Jussieu, 75252 Paris Cedex 05, France

Received August 15, 1989; revised April 16, 1990

Silica-supported hexamolybdate catalysts prepared by impregnation and two series obtained by calcination of the former are studied by different physicochemical techniques (IR and Raman spectroscopies, X-ray diffraction, and electronic microscopy) and tested in the catalytic oxidation of methanol. The nature of the surface species and the effect of water on the calcined catalysts are discussed as a function of the Mo loading (3 to 25 wt% Mo) from solid-state characterization and catalytic behavior. The catalysts unexposed to water (series 1) essentially exhibit a redox catalytic behavior, while the water-exposed catalysts (series 2) exhibit an acidic behavior. At high coverages ($\geq$10 wt% Mo), MoO_3 is the main species present on the surface. At lower coverages, a molybdenum oxo species is formed which is mainly responsible for the catalytic activity. This species is constituted of trimolybdic groups, fragments of the Keggin unit $SiMo_{12}$, in interaction with silica. Upon prolonged exposure to water, 12-molybdosilicic acid is also detected, but plays a minor role in the catalytic reaction.

INTRODUCTION

Polyoxomolybdates are anionic oxo-clusters which can be considered simplified oxide models. Because of their known nuclearity, dispersion on the support is expected to be better controlled. In our first investigations (*1*), performed with 12-molybdosilicic acid (Keggin structure cluster) supported on silica, we concluded that dispersion is an important parameter. At low coverages, an interaction can occur between the silica support and the catalytic species, leading to a modification of their catalytic behavior, tested in the oxidation of methanol.

In this paper, a smaller anion is used, the hexamolybdate $Mo_6O_{19}^{2-}$. As a tetrabutylammonium salt, this polymolybdate is stable in nonaqueous solvents, such as dimethylformamide, which enables control of the nuclearity of the deposit on the silica support. This control cannot be performed by using the usual starting material, ammonium heptamolybdate, because of the pH- and concentration-sensitive solution equilibria involving a variety of molybdate species. In the latter case, calcination treatments are generally carried out, leading to widely investigated Mo/SiO_2 catalysts (*2–15*). In spite of the wide attention given to these catalysts, their structure has given rise to much controversy. It is thus interesting to subject the silica-supported hexamolybdate samples to similar thermal treatments with the double object of studying the influence of the nuclearity of the deposit and of shedding more light on the nature of the Mo species present on the support. This paper deals with the study of Mo/SiO_2 catalysts prepared from hexamolybdate, including their solid-state characterization by different physicochemical techniques, and their catalytic behavior in the methanol oxidation reaction. The interest in this structure- and

0021-9517/90 $3.00

dispersion- sensitive test reaction has been already pointed out in previous works (Ref. (1) and references cited therein; Ref. (16)).

1. EXPERIMENTAL

1.1 Preparation of Samples

Hexamolybdate as tetrabutylammonium (TBA) salt was prepared according to a method previously described (*17*). Purity of $TBA_2Mo_6O_{19}$ was checked by thermogravimetry (TG) and by infrared and Raman spectroscopies.

The silica support (Rhône-Poulenc XOA 400, surface area 376 $m^2\ g^{-1}$) was dried under vacuum at 150°C for 10 h and then impregnated with dimethylformamide (DMF) solutions of $TBA_2Mo_6O_{19}$. Samples containing 3 to 25% of molybdenum (wt%) were prepared by stirring SiO_2 and impregnation DMF solutions under vacuum at room temperature. Complete elimination of the solvent was performed on the obtained powdered samples by heating at 170°C under vacuum for several hours (the absence of DMF was checked by IR spectroscopy). The final Mo content was determined by microanalysis techniques (Service Central de Microanalyse du CNRS, 69390 Vernaison, France).

Calcination of the samples was performed at 500°C for 6 h in air. Each calcined sample was divided into two parts: one part was kept in a closed tube while the other was exposed at room temperature to saturated water vapor ($P \sim 20$ Torr) overnight and for 2 days and then kept in a closed tube after air-stabilization. Calcined samples unexposed to water, referred to as I-500, II-500, etc., constitute series 1, and water-exposed calcined samples, referred to as I-500-W, II-500-W, etc., constitute series 2.

1.2. Physicochemical Techniques

1.2.1. Thermogravimetry (TG). Thermogravimetry was carried out in an air stream with a Perkin–Elmer TGA 7 thermogravimetric analyzer. Experimental conditions were as follows: sample weight 1 to 10 mg, heating rate 5°C per minute.

1.2.2. Infrared spectrometry (IR). Infrared spectra were recorded on a Perkin–Elmer 283 spectrophotometer (4000–200 cm^{-1}) and on a Perkin–Elmer FTIR 1700 interferometer (4000–450 cm^{-1}, scan number 10 to 20) as KBr pellets or as powder between two plates of KBr. Some measurements were performed on a Bruker 113 V FTIR interferometer (640–160 cm^{-1}, scan number 50) as RbI pellets.

1.2.3. Raman spectrometry. Raman spectra were run on a Coderg PHO spectrometer equipped with a Coherent Innova 70 argon laser (514.5 nm, 50 to 100 mW). Classical powder techniques were used, i.e., the capillary tube and the conical sample techniques. Low powers of the laser beam were used in order to avoid local reduction and/or destruction of the sample.

1.2.4. X-ray diffraction (XRD). X-ray diffraction patterns were obtained by reflection from powder packed in a sample holder with a SIEMENS D 500 diffractometer using the $CuK\alpha_1$ radiation.

1.2.5. Electron microscopy and X-ray analysis. Samples were observed by scanning electron microscopy with a JEOL TEM 100 CX apparatus (electron beam 200 Å in diameter, tension 100 kV). Micrographs were obtained from the secondary electrons reflected by the powder sample dispersed on a glue layer deposited on a platinum plate. Evaporating gold (150-Å layer) allows us to increase the contrast and to improve image quality. In addition, the X-ray beams, generated by the sample submitted to the beam of electrons, were analyzed with an energy dispersion analyzer LINK Model 10,000 (ultrathin window, 30-mm^2 monocrystal Si(Li) section). This technique allowed rough chemical analysis of the elements present on the surface. All the measurements were performed in the "Groupement régional de mesures physiques" (Université Pierre et Marie Curie, Paris).

1.2.6. Catalytic measurements. Oxidation of methanol was used as test reaction. The experimental conditions were similar to those already described in previous works (*16*). Catalytic activity and selectivity were

measured by using a continuous-flow fixed-bed reactor under atmospheric pressure. The catalyst was packed in a reactor of glass tubing (6 mm in diameter), placed in a vertical furnace, and preconditioned under oxygen at 140°C. The reagent mixture ($He/O_2/CH_3OH$) was admitted on the catalyst only after this temperature was reached. The optimized flow composition was 76.1/16.2/7.7 (mol%), corresponding to CH_3OH partial pressure of 58.2 Torr. This mixture was obtained by passing the He/O_2 flow through a methanol saturator maintained at 11.3°C. The catalyst weight (10 to 40 mg) and the flow rate of the reagent mixture were adjusted according to the conversion, which had to be kept lower than 8%, and according to the load loss at the level of the reaction zone, in order to be under the conditions of initial kinetics. The reaction was carried out at 230 and 250°C. Reaction products were analyzed on line by gas-phase chromatography, after stationary state was reached (after ~half-an-hour). Most of the experiments corresponding to stable activities and selectivities were conducted for several hours (in some cases 36 h). Selectivity (expressed in percent) for a product i was defined as the ratio between the number of MeOH moles transformed into i and the overall number of MeOH moles transformed during the same time. Activity A_i for the formation of a product i was calculated by

$$A_i = A_T \times S_i/100\, n_C,$$

with A_T total activity, i.e., overall number of MeOH moles transformed per hour and grams of Mo, S_i selectivity (%) for the product i, and n_C the number of C atoms in the product i.

2. RESULTS

2.1. *Hexamolybdate and Hexamolybdate/SiO_2 Samples*

The TG curve of $TBA_2Mo_6O_{19}$ shows that this compound is stable up to ~270°C. Breakdown of the organic cation and of the polyanion occurs, leading to MoO_3 at about 500°C, as checked by IR (theoretical weight loss 36.66%, experimental weight loss 36.73%). The IR and Raman spectra are consistent with those already published (*18*). The XRD powder diagram is shown in Fig. 1a.

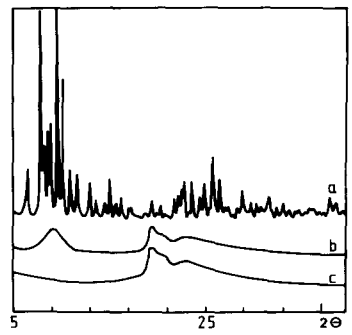

FIG. 1. XRD powder diagrams. (a) $TBA_2Mo_6O_{19}$; (b) sample III (7.1 wt% Mo/SiO_2); (c) silica.

Table 1 shows catalyst compositions of the five silica-supported hexamolybdate samples prepared by the impregnation method. TG curves of these samples exhibit weight losses corresponding to water departure (from room temperature) and breakdown of the organic cation (at temperatures shown in Table 1). It appears that the thermal stability of the supported catalysts is the same as that of the massic hexamolybdate within the experimental error.

IR spectra are shown in Fig. 2. Silica exhibits three main bands at ~1100 cm^{-1} (broad and very strong), ~800 cm^{-1} (medium), and ~470 cm^{-1} (strong). In addition, a weak band is observed at 976 cm^{-1} (this band disappears after prolonged treatment at 500°C and can be related to surface OH groups). The strongest bands of SiO_2 partly obscure the typical pattern of the hexamolybdate. Attempts to substract the absorption due to SiO_2 have been carried out: they were successful only for the high Mo contents (from 10% upward). This can be understood when the strong 1100-cm^{-1} SiO_2 band, whose width and shape are not favorable for difference treatments, is considered. This band is very sensitive to sampling conditions and to hygroscopic degree. Even with low concentrations of SiO_2 in KBr (absor-

TABLE 1

Characteristics of Silica-Supported Hexamolybdate Samples

Sample	wt% Mo init.	wt% Mo exp.	wt% Si init.	wt% Si exp.	Massic ratio Mo/SiO_2	T(°C) dec.[a]
I	24.0	25.0	20.0	15.4	0.758	~270
II	16.8	17.4	28.0	27.7	0.293	~270
III	10.5	7.1	35.0	31.6	0.105	~260
IV	6.0	5.4	40.0	35.6	0.071	~260
V	3.2	3.1	45.0	40.8	0.035	~260

[a] dec. indicates decomposition.

bances less than one), it is practically impossible to perform satisfactory differences of spectra of two different KBr pellets of pure silica. When the bands due to the molybdenum species are important with respect to those of the SiO_2 substrate, modifications of the latter are negligible, and differences can be realized. This is no longer possible at low Mo contents because the signals are very weak with respect to those of the substrate: differences between two inaccurate data are obtained with a high error, leading to artifact bands. These considerations prevented us from performing difference treatments. Then, from the original IR spectra, hexamolybdate was characterized without ambiguity for compounds I to III. For compounds IV and V, only the high-frequency 956-cm^{-1} IR band was detected.

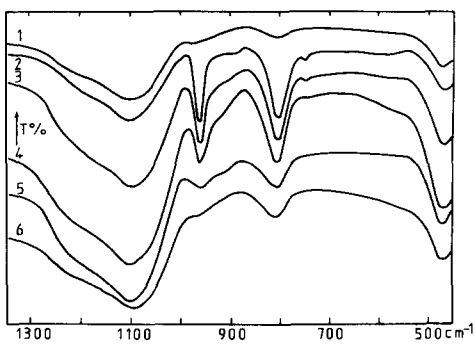

FIG. 2. IR spectra of silica and silica-supported hexamolybdate samples. (1) silica; (2) I; (3) II; (4) III; (5) IV; (6) V.

Raman spectra show a hexamolybdate pattern (*18*) for compounds I and II, a high-frequency 989-cm^{-1} band for compounds III and IV, and no signal for compound V. However, silica does not give any peak, hindering polymolybdate detection. The relatively poor quality of the Raman spectra is probably due to the bad crystallinity of the supported samples (no fluorescence background).

Indeed, this poor crystallinity is evidenced by XRD measurements. The diagrams do not exhibit any lines of crystalline phase. Only a broad peak is observed, centered at the same position as the strongest of the crystalline $TBA_2Mo_6O_{19}$ (e.g., sample III in Fig. 1b). X-ray analysis is not a suitable characterization method for these impregnated catalysts: it appears that impregnation induces amorphization of the deposit on the support.

From electron microscopy measurements, it appears that silica is composed of spheres of variable sizes, as shown in Fig. 3a. For the impregnated samples, crystalline forms are never observed. Only the samples with low Mo contents exhibit relatively regular dispersion of aggregates. For the high Mo contents, heaps and aggregates of variable sizes are irregularly deposited on the silica surface, with relatively bare zones between the aggregates.

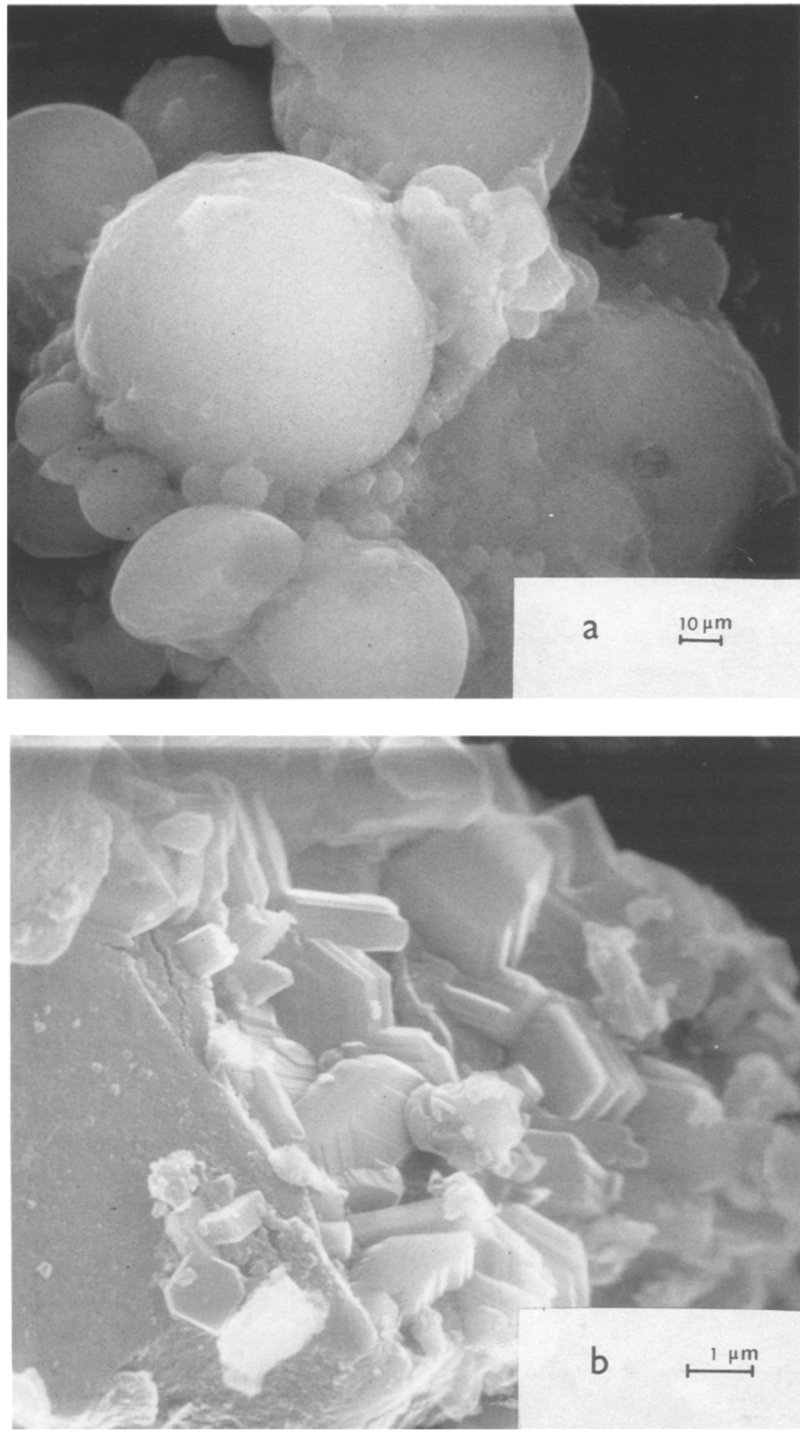

FIG. 3. Electron micrographs. (a) Silica; (b) I-500-W; (c) III-500-W; (d) V-500-W.

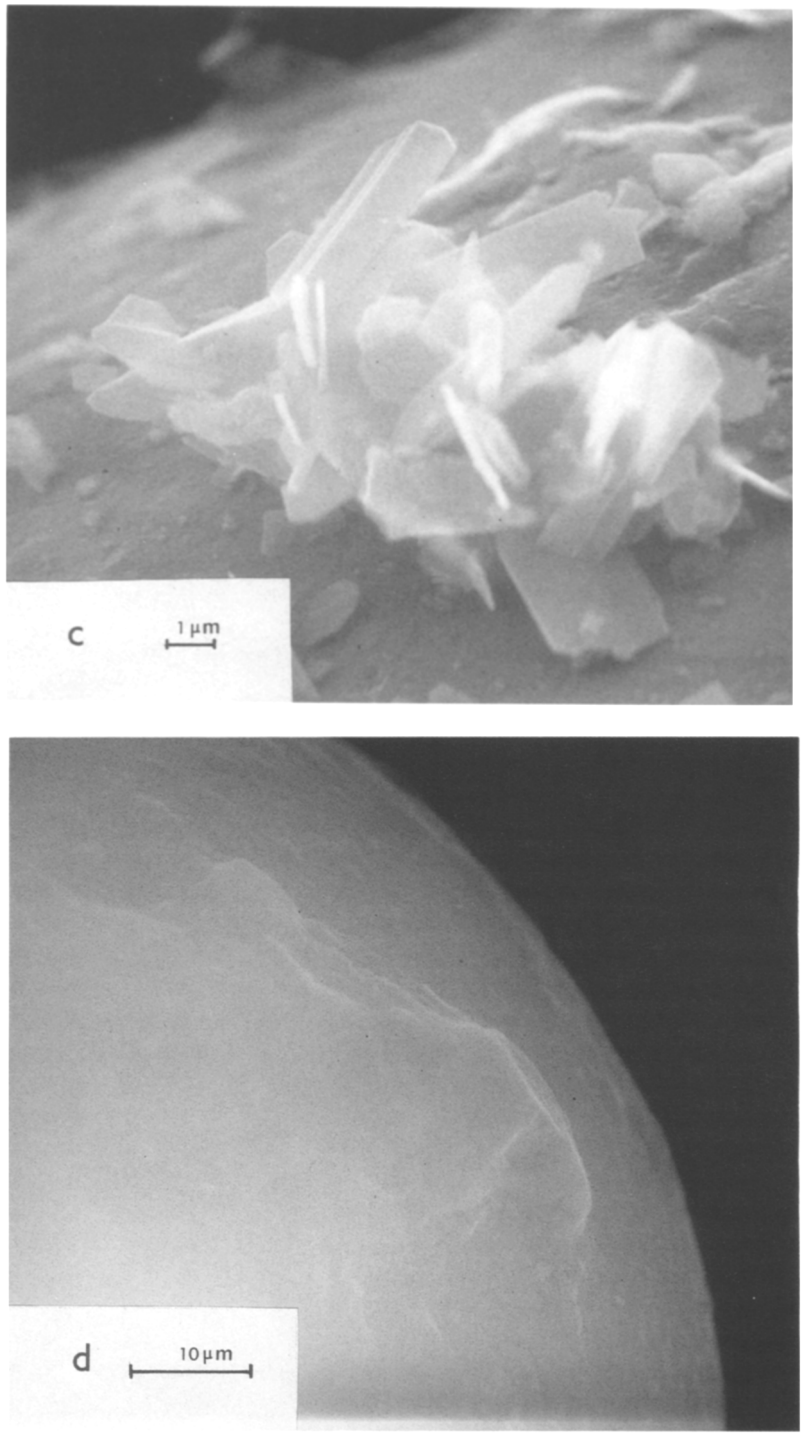

FIG. 3—*Continued*

The impregnated samples were tested in the methanol oxidation reaction. The samples were brought to 230°C (temperature lower than that of decomposition) under gas flow without giving any activity. Prolonging the thermal treatment overnight at this temperature induces activity, which, however, rapidly decreases upon reduction and loss of the catalytic species (blue Mo deposit on the walls of the glass reactor).

From these results, it appears that the hexamolybdate/SiO_2 samples are not suitable in the test reaction of methanol oxidation. However, when subjected to thermal treatments in order to decompose the organic cation and the hexamolybdate, they can be used as Mo/SiO_2 catalysts. The large TBA cations maintain the anions far from each other: collapse of the anions could be expected to be performed without diffusion of the Mo atoms, giving rise to small heaps of the same nuclearity as that of the hexamolybdate precursor.

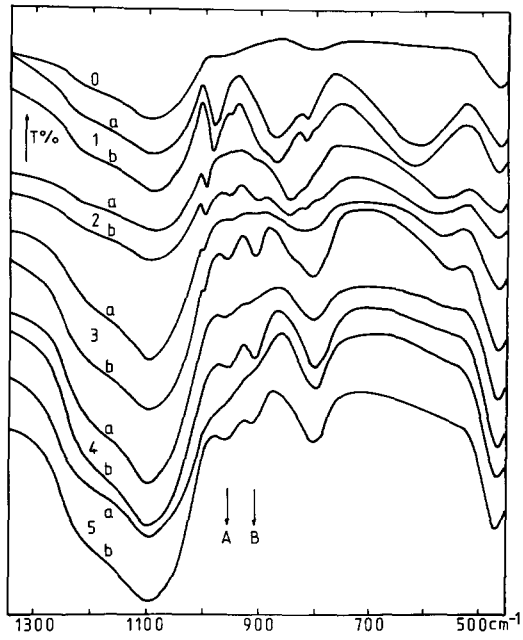

FIG. 4. IR spectra of calcined Mo/SiO_2 catalysts. (0) silica; (1a) I-500; (1b) I-500-W; (2a) II-500; (2b) II-500-W; (3a) III-500; (3b) III-500-W; (4a) IV-500; (4b) IV-500-W; (5a) V-500; (5b) V-500-W.

2.2. *Calcined Catalysts*

Activation of the hexamolybdate/SiO_2 samples has been performed under conditions usually used by other research groups to obtain Mo/SiO_2 catalysts from different precursors. Thermal treatments have been carried out according to the conditions developed in Section 1.1. (compounds of series 1). Moreover, according to several authors (*3–5*), water is expected to modify the nature of the species on the surface, and, consequently, to play a role in catalytic behavior. Therefore, a part of these samples has been exposed to saturating water vapor (compounds of series 2: see Section 1.1.). The weight increase due to water absorption varies from 15 to 22%.

2.2.1. IR spectra. IR spectra of the samples are shown in Fig. 4. As in the case of the hexamolybdate/SiO_2 samples, the shape and the maximum frequency of the strong 1100-cm^{-1} SiO_2 IR band undergo modifications related to the state of silica and to interactions between the support and the deposit. It is the reason why only original spectra, and not difference spectra, are examined to characterize the nature of the deposit.

IR bands (referred to as a, b, c, d, and e in Table 2) of a species closely related to orthorhombic MoO_3 are observed for compounds I to III (500 and 500-W). Frequency shifts, particularly important for bands b and d (both strong and broad) of compounds II and III (500 and 500-W) could be related to modifications in the three-dimensional framework of orthorhombic MoO_3, the structure of which is preserved as a whole. For the low Mo contents (compounds IV and V, 500 and 500-W), no MoO_3 is detected. In addition, all the water-exposed compounds (series 2) exhibit two other bands at 955–957 cm^{-1} (band A) and 902–914 cm^{-1} (band B), which always appear simultaneously. These bands are seen as shoulders in the spectra of series 1 samples, probably because adsorption of atmospheric water is sufficient to generate the

TABLE 2

IR Frequencies (cm^{-1}) of MoO_3 in the Calcined catalysts

Sample	*a*	*b*	*c*	*d*	*e*
MoO_3[a]	994	862	818	590	368
	s	vs	w	vs	s
MoO_3[b]	1000	865	820	600	375
	s	vs	w	vs	s
MoO_3[c]	993	872	819	570	375
	s	vs	w	vs	s
I-500	986	872	818	618	370
	s	vs	w	vs	m
I-500-W	987	877	818	623	370
	s	vs	w	vs	m
II-500	1000	847	821	561	370
	m	s	w	s	w
II-500-W	999	852	821	583	370
	m	s	w	s	w
III-500	1002	838	821	565	365
	w	m	vw	m	w
III-500-W	1002	842	821	558	368
	w	m	vw	m	w

Note. Intensity: vs, very strong; s, strong; m, medium; w, weak. Width: bands a and e, narrow;bands b and d, broad.

[a] Commercial grade (Prolabo).

[b] Commercial grade, ground and water exposed.

[c] Sublimated at 800°C.

species. The origin of bands A and B will be discussed below. In the low-frequency region, no bands are observed, except those characteristic of MoO_3 for compounds containing this oxide.

2.2.2. Raman spectra. Orthorhombic MoO_3 (see Table 3) is detected in the Raman spectra of all the samples except IV-500, V-500, and V-500-W (no signals for these three samples, which exhibit no fluorescence background). Water-exposed samples give more intense signals, and, generally, spectra of better quality. Raman spectroscopy is very sensitive in detecting organized MoO_3, which is characterized by highly intense signals. The frequencies of the supported MoO_3 are almost identical with those of the bulk MoO_3, except in the low-frequency region, indicating some modifications in the framework. Such modifications were also evidenced by IR spectrometry, as pointed out above. The supported MoO_3 probably weakly interacts with the silica support. For the very low Mo contents, there are not enough Mo centers to constitute repetitive units on a range long enough to characterize organized MoO_3. Additional bands characteristic of one or several Mo oxo species are detected in the spectra of III-500-W and IV-500-W exposed to water for 2 days (when exposed only overnight, no signals are detected); Raman spectra of these two samples are shown in Fig. 5. These additional bands will be discussed below.

2.2.3. X-ray diffraction. Results obtained by XRD show that orthorhombic MoO_3 (*19*) is detected in samples I to III (500 and 500-W). For the water-exposed samples (series

TABLE 3

Raman Frequencies (cm^{-1}) of MoO_3 in the Calcined Catalysts

MoO_3[a]	994	820	665	382 368	338	292 285	248	219	198	158	129	115
MoO_3[b]	995	819	665	378	336	290	244	216	197	156	128	115
I-500	994	820	665	380	339	282	240	215	196	150	127	115
I-500-W	993	820	663	375	335	280	236	210	193	150	125	110
II-500	995	820	665	Difficult to obtain								
II-500-W	995	820	665	377	337	285 282	240	210	195	150	125	110
III-500	995	820	670	376	338	285	240					
III-500-W[c]	994	820	667	380	339	292 285	245	218	198	158	130	118
IV-500				No band								
IV-500-W[c]	994	820	665	370	340	295						
V-500				No band								
V-500-W				No band								

[a] Commercial grade (Prolabo).
[b] Sublimated at 800°C.
[c] Additional bands not due to MoO_3 (see Fig. 5) are discussed in the text.

2), formation of a hydrate of molybdenum oxide could be expected. The dihydrate $MoO_3 \cdot 2H_2O$ (so-called yellow molybdic acid) has been described as monoclinic (*20*). The presence of such a compound is, however, not evidenced. Some typical patterns are presented in Fig. 6. XRD technique is less sensitive than Raman spectroscopy: the X-ray pattern of MoO_3 can only be detected on samples with Mo content $\geq 7\%$, whereas the Raman spectrum of IV-500-W (Mo content 5.4%) clearly shows the presence of MoO_3. At this level, either the particles are amorphous, or the crystalline domains are too small to give rise to a XRD pattern. Small shifts of the more intense diffraction lines (101, 400, and 210) are observed for the water-exposed samples. The effect of water exposure is shown in Table 4, comparing the results of MoO_3, III-500, and III-500-W. The shifts can be related to small modifications of the orthorhombic unit cell, favored by exposure to water. Pure silica gives only broad lines typical of a noncrystalline material (Figs. 1c and 6f). This pattern of silica is detected for the supported samples, with slight modifications in the case of water-exposed samples. In addition, a noncrystalline species (weak broad band at *d* (interplanar spacing) ~10 to 11 Å) is observed in the patterns of all the water-exposed samples (even those without orthorhombic MoO_3), but is absent for the samples unexposed to water (*21*).

2.2.4. Electron microscopy. Electron microscopy allows the detection of crystalline Mo species for samples I to III (500 and 500-W). These species appear as long plates, isolated or gathered as aggregates similar to classical orthorhombic MoO_3 crystals. Some of these aggregates resemble a rose in shape. Water effect is not evidenced on the micrographs (no significant differences between the samples of series 1 and 2). Evident surface heterogeneity is seen, especially for the middle Mo content samples (e.g., III-500

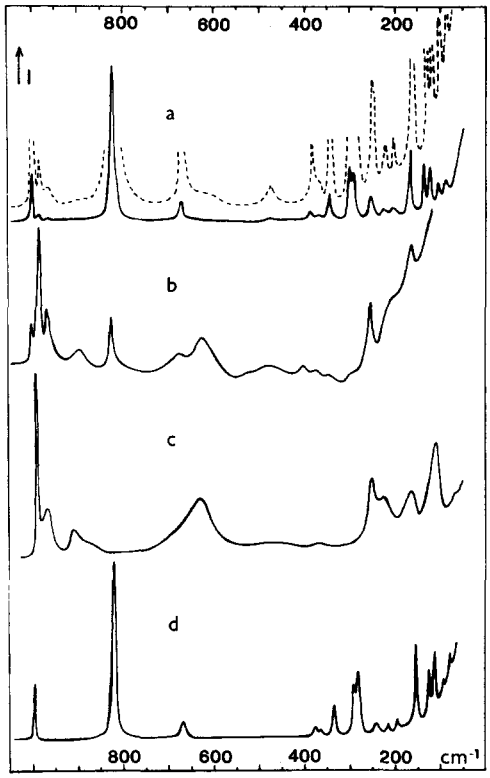

FIG. 5. Raman spectra of water-exposed catalysts (MoO_3 + additional species), 12-molybdosilicic acid, and MoO_3. (a) III-500-W (dotted line expanded seven fold); (b) IV-500-W; (c) 12-molybdosilicic acid (according to Ref. (*24*), powdered sample pressed in a matrix and rotated at about 1000 rpm); (d) MoO_3.

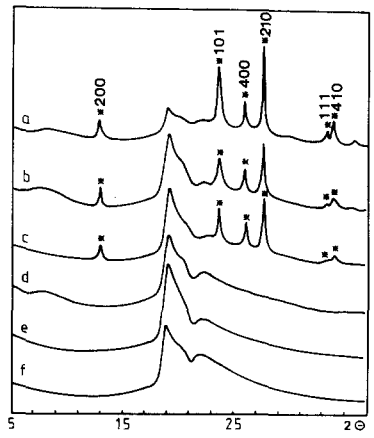

FIG. 6. XRD powder diagrams of some silica-supported calcined catalysts (lines marked with an asterisk are characteristic of MoO_3). (a) II-500-W; (b) III-500-W; (c) III-500; (d) IV-500-W; (e) IV-500; (f) SiO_2.

and III-500-W), with relatively large barren zones. For samples with low Mo content (e.g., IV-500 and IV-500-W), heaps of different sizes are visible; these are probably fragments of the background, according to X-ray analyses, showing a Mo/Si ratio roughly constant at different points of the surface. However, these analyses must be considered with caution because of the low Mo content, which requires high amplification of the signal with, consequently, high noise and poor precision and because of the beam width. Some typical micrographs are shown in Fig. 3.

2.2.5. Catalytic behavior of silica-supported Mo samples. All the calcined samples were tested at 230 and 250°C in the methanol oxidation test reaction. All the results are gathered in Tables 5 and 6. Selectivities for the different products of transformation of methanol are shown in Figs. 7 and 8. Each point is the mean of several experiments performed at similar conversions (Tables 5 and 6). Activities, shown in Fig. 9, are expressed with respect to the molybdenum weight (number of MeOH moles transformed per hour and per 1 g of Mo) in order to obtain a direct relation between the methanol transformation and the amount of Mo deposited on the support.

Redox catalysis is predominant for the samples unexposed to water (series 1). Formaldehyde is the main product for samples I-500 to IV-500, as for massic MoO_3 (*22*). A decrease in formaldehyde selectivity is observed for V-500, paralleled with an increase in methyl formate selectivity (Fig. 7). In addition, production of dimethyl ether is weak whatever the Mo content and seems to be decreasing at low coverages.

In contrast to the above results, acidic catalysis is predominant for the water-exposed samples (series 2): dimethyl ether is the main product formed, whatever the reaction temperature. The selectivity for dimethylether does not vary as a function of

TABLE 4

Interplanar Spacings d_{hkl} (Å) and Relative Intensities *I*% of MoO_3 and Some Calcined Catalysts

hkl	MoO_3 theor.[a]	MoO_3 exp.	*I*%	II-500-W	*I*%	III-500-W	*I*%	III-500	*I*%
101	3.810	3.809	48	3.739	77	3.805	77	3.813	81
400	3.464	3.462	60	3.451	46	3.459	65	3.465	66
210	3.261	3.264	100	3.249	100	3.258	100	3.265	100

[a] Ref. (*19*).

time: it remains constant even after 36 h of reaction at 230°C. The acidic character decreases at low coverages, with increase in selectivity for formaldehyde (Fig. 8). In contrast to the results obtained with $SiMo_{12}H/SiO_2$ catalysts (*1*), for which the selectivity for methyl formate strongly increases when the Mo loading decreases, this selectivity is very weak for all the samples of series 2.

Activity of the samples of series 1 decreases as the Mo content increases. At high coverages, heaps of orthorhombic MoO_3 are piled up over the surface, with just a few active centers available for the reaction, exactly as for massic MoO_3, which is known to present a low activity toward methanol conversion (*22*). Decreasing the Mo coverage leads to better accessibility to the active sites and favors the catalytic reaction. This activity is always relatively weak with respect to that of the samples of series 2. It is worth noting that the enhanced activity of the latter is essentially due to the acidic catalytic character. However, the redox activity of the samples of series 2 (Fig. 9) is about three- to fivefold higher than that of the samples of series 1. It increases with decrease in the Mo content and tends to slightly decrease at the lowest coverage, in contrast

TABLE 5

Selectivities and Activities of Catalysts Unexposed to Water (Series 1)

Sample	*T*(°C)	Mo/SiO_2 Massic ratio	Selectivities (%)					Total activities (mmol/h/g Mo)	Conversion (%)
			1	2	3	4	5		
I-500	250	0.758	50	22	14	13	1	32	8
I-500	230	0.758	40	17	30	12	1	23	5.5
II-500	250	0.293	51	22	15	11	1	51	6
II-500	230	0.293	45	21	24	9	1	34	4
III-500	250	0.105	52	22	18	7	1	57	2.5
III-500	230	0.105	42	24	26	6.5	1.5	47	2
IV-500	250	0.071	49	43	6	1	1	87	4.5
IV-500	230	0.071	42	25	26	5	2	77	2.5
V-500	250	0.035	26	59	11.5	1.5	2	135	3.5
V-500	230	0.035	30	31.5	33	3.5	2	92	3

Note. 1, CH_2O; 2, $HCOOCH_3$; 3, $(CH_3O)_2CH_2$; 4, $(CH_3)_2O$; 5, CO_2 + CO.

TABLE 6

Selectivities and Activities of Water-Exposed Catalysts (Series 2)

Sample	T(°C)	Mo/SiO_2 Massic ratio	Selectivities (%)					Total activities (mmol/h/g Mo)	Conversion (%)
			1	2	3	4	5		
I-500-W	250	0.758	27	3	9	60	1	205	8.5
I-500-W	230	0.758	21	3	18	57	1	123	6
II-500-W	250	0.293	18	1.5	13	67	0.5	418	7
II-500-W	230	0.293	19	3	20	57	1	272	6.5
III-500-W	250	0.105	15	3	8	73	1	1012	7
III-500-W	230	0.105	10	2.5	12	75	0.5	690	7
IV-500-W	250	0.071	15	4	10	70	1	744	4.5
IV-500-W	230	0.071	13	3	17.5	66	0.5	524	4.5
V-500-W	250	0.035	23	7	29	40	1	406	4.5
V-500-W	230	0.035	16	3	34	46	1	314	3.5

Note. 1, CH_2O; 2, $HCOOCH_3$; 3, $(CH_3O)_2CH_2$; 4, $(CH_3)_2O$; 5, CO_2 + CO.

to the results obtained with the samples of series 1. At high coverages, a decrease in activity is due to piling up of heaps of MoO_3, as for the samples of series 1.

The possibility of structural change of catalysts of series 1 under the action of water formed by the reaction has been envisaged. Under this assumption, the activities of both series ought to be the same: this is not the case. When an effect of water on the catalysts of series 1 during the reaction is assumed, at least a tendency to increase activity for dimethylether ought to be observed: activities are not time dependent, which is not consistent with the hypothesis. This eventuality must then be rejected. This is perhaps because the conditions are completely different: at room temperature, water acts in the liquid phase at the solid/liquid interface, while at the reaction temperature (230 or 250°C), it acts in the vapor state at the solid/gas interface, where rapid desorption likely occurs. Moreover, $P(H_2O)$ under reaction working conditions is much weaker than saturated $P(H_2O)$ at room temperature.

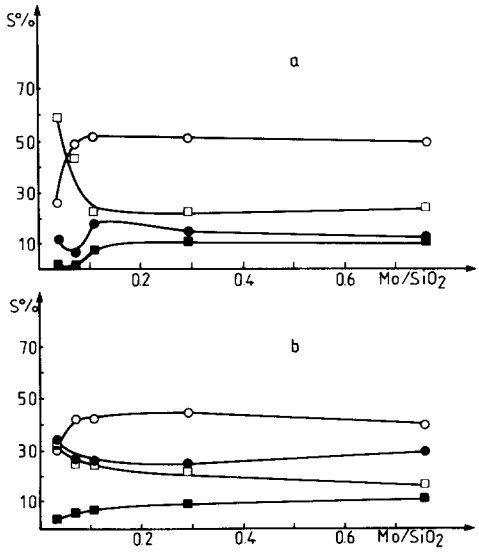

FIG. 7. Selectivities (expressed in percent) of the catalysts of series 1 versus Mo loading (a: 250°C; b: 230°C). (○) CH_2O; (□) $HCOOCH_3$; (●) $(CH_3O)_2CH_2$; (■) $(CH_3)_2O$.

3. DISCUSSION

3.1. The Nature of the Mo Species as a Function of Mo Loading

We have developed in the above paragraphs the results of our investigations on silica-supported catalysts prepared from

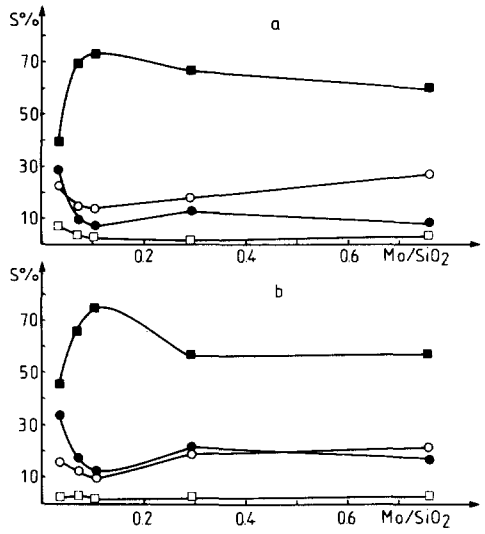

FIG. 8. Selectivities (expressed in percent) of the catalysts of the series 2 versus Mo loading (a: 250°C; b: 230°C). (○) CH_2O; (□) $HCOOCH_3$; (●) $(CH_3O)_2CH_2$; (■) $(CH_3)_2O$.

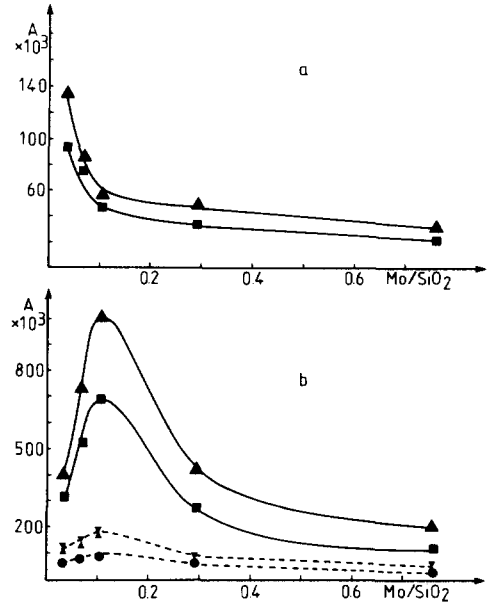

FIG. 9. Activities (mol/h/g Mo) of the calcined Mo/SiO_2 catalysts versus Mo loading. (a) Series 1; (b) series 2; full lines, total activity. (▲, 250°C; ■, 230°C); dotted lines, redox activity (⧗, 250°C; ●, 230°C).

hexamolybdate. It is now worth reviewing the results already published, obtained by a number of research teams on molybdenum catalysts supported on SiO_2 and/or γ-Al_2O_3 (*2–15*).

Ammonium heptamolybdate was generally used as a starting material. Catalysts were prepared by the conventional pore volume impregnation of SiO_2 and/or γ-Al_2O_3 supports, using aqueous solutions of various concentrations, followed by drying at 110–130°C and calcination in air at 500°C for several hours.

The effect of Mo content on the nature of the species on the surface of these Mo catalysts has been discussed on the basis of various physicochemical techniques such as X-ray diffraction (*2–4, 8, 14*), UV-visible diffuse reflectance (*3, 4, 8*), Raman spectrometry (*4–6, 10, 13–15*), IR spectrometry (*7, 9, 12, 14, 15*), etc.

From these results, several ranges can be defined, depending on the Mo loadings (high, medium, or low). The limits between the different ranges depend on the techniques used to characterize the surface species.

At high Mo loadings (>15% Mo), all the authors agree on the presence of "free" MoO_3, which can be considered equivalent to massic MoO_3. At intermediate Mo loadings, MoO_3 is detected together with other undefined Mo species, generally designated as polymolybdates. At low Mo loadings (a few percent), several oxo-Mo species are postulated, and named "pseudomolybdates" (*12*), polymolybdates (*4–6, 8, 10, 12–14*), surface molybdate (*11*), surface polymer molybdate (*6a, 7, 8c*), heptamolybdate (*15*), or silicomolybdic acid (*3, 4, 9, 10, 15*).

We have also shown the presence of MoO_3 on our samples at Mo loadings higher than ~5% by XRD, IR, and Raman spectra, and scanning electron microscopy. Some modifications with respect to bulk MoO_3 have been reported in the above paragraphs and could be related to weak interactions with the support. Such interactions

have also been suggested according to the modifications of the intensities of the XRD lines (*8*).

3.2. Earlier Assignments of IR Bands at ~960 and ~910 cm^{-1}

Whatever the Mo content, two bands at 955–957 cm^{-1} and 902–914 cm^{-1}, not characteristic of MoO_3 and referred to as A and B are simultaneously observed in the IR spectra of our samples (Fig. 4). These bands are more marked for the water-exposed samples.

Similar bands (at 910 and 960 cm^{-1}) have been observed by Goncharova *et al.* (*9*) on a Mo/SiO_2 catalyst with 3.8 wt% Mo. The authors consider that they are due to silicomolybdic acid formed during the preparation of the catalyst. This interpretation implies enhanced thermal stability of the $SiMo_{12}O_{40}^{4-}$ anion (abbreviated $SiMo_{12}$) when supported on silica. Similarly, Kasztelan *et al.* (*15*) suggest that silicomolybdic acid (abbreviated $SiMo_{12}H$) is synthesized during the impregnation of the Mo/SiO_2 catalysts (~2 wt% Mo at pH 2, 7, and 11) and that the silica support stabilizes this species which remains predominant after calcination at 500°C. These statements of higher stability are not consistent with our recent work on the thermal behavior of $SiMo_{12}H/SiO_2$ catalysts, from IR and catalytic reactivity studies (*23*).

Seyedmonir *et al.* (*7*) observe three bands (994, 970, 925 cm^{-1}) due to oxomolybdenum species in the IR spectrum of a Mo/SiO_2 catalyst (6 wt% Mo). The first band (994 cm^{-1}) is assigned to MoO_3. The second (970 cm^{-1}) is assigned to terminal Mo=O vibrations of a polymeric surface polymolybdate phase, assignment supported by similar results in the Raman study of calcined Mo/SiO_2 catalysts (*6a, 8c*). Other authors have also observed bands at 950–960 cm^{-1}, attributed to terminal Mo=O stretchings of surface polymolybdate (*4b, 11, 13, 14*).Last, the 925-cm^{-1} band is tentatively assigned to a Si–O–Mo vibration. As a support of this assignment, it is recalled that the stretching vibration of the SiO_4 tetrahedron in $SiMo_{12}$ occurs at ~910–920 cm^{-1}, with strong coupling with Mo–O vibrations (*24*).

Such an assignment of a band at 920 cm^{-1} to Si–O–Mo vibration is made by Cornac *et al.* (*12*) in a FTIR study of Mo/SiO_2 catalysts. For a sample with 2 wt% Mo, the authors postulate the presence of a pseudomolybdate with Mo = O stretching at 990 cm^{-1}. At higher Mo content (8 wt%), an additional band is observed at 970 cm^{-1}, attributed to a polymolybdate.

It appears thus that the set of two IR bands at 960–970 cm^{-1} and 910–920 cm^{-1} has received contradictory assignments.

3.3. UV-Visible Diffuse Reflectance Spectroscopy (DRS) *in Connection with the Presence of Silicomolybdic Acid*

A similar situation occurs with UV-visible diffuse reflectance spectroscopy, a technique commonly used to determine the symmetry and the environment of transition metal ions in supported oxide catalysts. From this technique, Marcinkowska *et al.* (*4a*) postulate the presence of $SiMo_{12}H$, destroyed at 500°C and rebuilt with water vapor at room temperature on Mo/SiO_2 catalysts at low Mo loadings, a statement apparently confirmed by Raman measurements (*4c*). However, Gajardo *et al.* (*8*) do not find evidence supporting the presence of $SiMo_{12}H$ on the Mo/SiO_2 catalysts by UV-visible DRS: they concur with the presence of a surface species similar to a polymolybdate. However, a recent work (*25*) on the UV-visible DRS of model polyoxomolybdates with known structures shows that the above interpretations rest upon attributions which must be reconsidered: indeed, UV-visible DRS cannot give evidence for the presence of a given polyoxomolybdate; it only gives information about the size and the dispersion of the clusters.

3.4. Postulated Existence of $SiMo_{12}H$

At this point in the discussion, several questions can be raised: Can $SiMo_{12}H$ exist or be formed on a silica support at a temper-

ature as high as 500°C (bulk $SiMo_{12}H$ is destroyed at about 300–330°C)? What are the proofs for its existence? What is the role of water?

Castellan *et al.* (*3*) and Barbaux *et al.* (*10*) use acidimetric titrations to evidence the existence of $SiMo_{12}H$ on the Mo/SiO_2 catalysts at low Mo loadings. Their results are not fully conclusive, since the extraction process migh favor the formation of the $SiMo_{12}H$ species in the solution because of the solubilization of oxo-Mo species and silica at a pH low enough, thanks to the acidic character of the silica support. To substantiate this statement, we have performed the following experiment: MoO_3 and SiO_2 were separately stirred in water for several days. The insoluble matter was filtered off, and the two filtrates were mixed (resulting pH ~2.5). After evaporation to dryness, the IR spectrum was consistent with a mixture of silica and 12-molybdosilicic acid.

The same comment can be made about the experiments performed by Kasztelan *et al.* (*15*) who wash Mo/SiO_2 catalysts in acetonitrile solution. IR and Raman spectra are given to support the presence of $SiMo_{12}H$ in CH_3CN solution, and, therefore, on the solid.

The same authors (*15*) and Barbaux *et al.* (*10*) also report Raman measurements in the solid state, an approach which does not suffer from the previously mentioned defects. The former (*15*) claim to clearly distinguish the characteristic bands of $SiMo_{12}H$ on Mo/SiO_2 catalysts (2 w% Mo, pH 2 and 7): however, the whole pattern of $SiMo_{12}H$ is not seen, and only a band at 985 cm^{-1} can be associated with this species. The latter (*10*) observe only a broad and weak band at 980 cm^{-1} ascribed to $SiMo_{12}H$, for Mo/SiO_2 catalysts with 1 and 3.8 wt% Mo. This Raman band, together with the acidimetric titrations and the yellow color of the samples, is taken as evidence of $SiMo_{12}H$. It may be appropriate to mention that the yellow color is also developed by the dihydrated molybdenum oxide (*20*) and the hexamolybdate, the precursor of our samples: all the compounds that are yellow are not necessarily silicomolybdic acid.

In the work of Kasztelan *et al.* (*15*) and Barbaux *et al.* (*10*), the formation of $SiMo_{12}H$ does not appear to be related to the presence of water. Rodrigo *et al.* (*11*) report as well a Raman study on Mo/SiO_2 catalysts without special exposure to water: $SiMo_{12}H$ can be detected (bands at 980 and 950 cm^{-1}) at loadings as low as 1% Mo. In all these cases (*10, 11, 15*), however, samples are handled in air, without special care against atmospheric water. It is possible that the oxo-Mo species responsible for the 980-cm^{-1} Raman band is formed from atmospheric water adsorbed on the silica support. This assumption is supported by controlled atmosphere Raman measurements (*4c*) including cycles of calcination at 500°C followed by introduction of water vapor. Bands at 980 and 950 cm^{-1} assigned to $SiMo_{12}H$ are present only after introduction of water into the cell (4% Mo/SiO_2 catalyst). The species is expected to be destroyed at 500°C and rebuilt at room temperature upon water exposure. This water effect, which could depend on the nature of silica (porosity, surface area), is certainly a fundamental parameter in the results observed with these Mo catalysts.

3.5. Nature of the Mo-Oxo Species from IR and Raman Spectra and from Catalytic Behavior

We now must interpret the origin of the two bands A and B observed in the IR spectra of our catalysts. The above discussion about the water effect is consistent with the first conclusions already proposed above. These bands are due to a species which needs water in order to be formed. It exists only in small amounts in samples of series 1 which have been in contact with atmospheric water. It is a surface species, which can exist even at high Mo loadings. In this case, the predominant species, MoO_3, is not uniformly covering the surface, according to electron microscopy results. So accessibility to bare silica surface, on which the

Mo species can interact, is possible. *The frequencies of bands A and B (respectively 955–957 cm^{-1} and 902–914 cm^{-1}) are consistent at least with the presence of a polymolybdate phase in interaction with silica.*

The possibility of the presence of $SiMo_{12}H$ is supported by only two characteristic IR bands: the 800-cm^{-1} band can be obscured by the SiO_2 support contribution, and the others are perhaps too weak to be detected. The Raman spectra do not give evidence for the presence of $SiMo_{12}H$, except for samples III-500-W and IV-500-W, which will be discussed below.

With the general point of view of a polymolybdate phase, band A corresponds to the Mo=O stretching of the polymolybdate. Among all the known polymolybdic species, only those containing the trimolybdic group Mo_3O_{13}, constituted of three MoO_6 octahedra sharing edges, exhibit a Mo terminal O band at such a frequency. These trimolybdic groups, common to well-known polymolybdates (e.g., $SiMo_{12}$ of Keggin structure or $Mo_6O_{19}^{2-}$ of Lindqvist structure), are characterized by "group frequencies," in particular by an IR band at 955–960 cm^{-1} (asymmetric stretching of Mo terminal O bonds) (*26*). *We therefore suggest that all the samples contain a polymolybdate phase constituted at least of trimolybdic groups connected together and to the silica support.* This interaction with silica gives rise to Si–O–Mo stretching at 900–910 cm^{-1} (band B).

The scheme of formation of the trimolybdic groups can be understood by considering that water can favor the transformation of the molybdenum oxide (species formally written MoO_3, irrespective of its organization), according to

$$3MoO_3 + 4H_2O \rightarrow [Mo_3O_{13}H_8].$$

This condensed species can react with silica, with water release, to give

$$[Mo_3O_{13}H_8] + SiO_2 \rightarrow [Mo_3O_{13}H_6\text{—}O\text{—}Si] + H_2O.$$

Such a surface Mo-oxo species would be highly acidic. In the case of further condensation favored by water action, formation of Keggin units by such a repetitive process could be possible if the duration of water exposure is sufficient.

We have already pointed out that this duration induces spectroscopic changes: in addition to MoO_3 bands, Raman bands observed for samples III-500-W and IV-500-W only appear after water exposure for 2 days (see Fig. 5). These bands at ~980, 960, and 625 cm^{-1} are consistent with the presence of either trimolybdic groups or $SiMo_{12}H$. These two possibilities are not in contradiction, since the trimolybdic groups are fragments of $SiMo_{12}$. In both cases, assignments are as follows (*26*): 980 cm^{-1} (symmetric stretching of Mo terminal O bonds), 960 cm^{-1} (asymmetric stretching of Mo terminal O bonds), 625 cm^{-1} (symmetric stretching of Mo bridging O–Mo). The low-frequency region is partly obscured by MoO_3 bands: however, the 245-cm^{-1} band, *partly due to MoO_3*, can be related either to Si–O–Mo bending or to the presence of $SiMo_{12}H$. The general shape of the Raman bands, especially for IV-500-W, is rather in favor of $SiMo_{12}H$. However, the frequencies are not the same as in bulk $SiMo_{12}H$ (see Ref. (*24*) and Fig. 5c) (980 instead of 988 cm^{-1}, 960 instead of 963 cm^{-1}, 625 instead of 634 cm^{-1}). These frequency shifts could be interpreted in terms of dispersion and/or interaction effects with the support (such decreasing of frequencies has already been interpreted in terms of weakening of anion–anion interactions (*24*)).

It is now of great interest to compare the catalytic behavior of the samples of series 2 and those prepared by direct impregnation of $SiMo_{12}H$ on silica (*1*) (Fig. 10 and Table 7). The selectivities for both kinds of catalysts present some similarities, although the formation of dimethylether is significantly more important for series 2 samples at low Mo content, in contrast with that of methyl formate which is significantly lower. Concerning the activities, different behaviors are observed: for low Mo contents, activi-

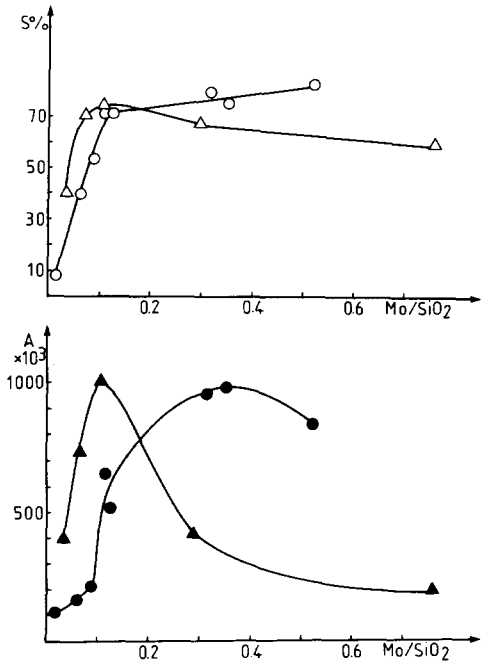

FIG. 10. Comparison of the selectivities for dimethylether and total activities (mol/h/g Mo) of the series 2 and $SiMo_{12}H/SiO_2$ catalysts (at T = 250°C). Series 2 catalysts: (△) selectivity for $(CH_3)_2O$; (▲) total activity. $SiMo_{12}H/SiO_2$ catalysts: (○) selectivity for $(CH_3)_2O$; (●) total activity.

TABLE 7

Selectivities and Activities of $SiMo_{12}H/SiO_2$ Catalysts (T = 250°C)

Mo/SiO_2[a]	Selectivities (%)				Total activity (mmol/h/g Mo)
	1	2	3	4	
0.522	10	2	5	83	841
0.352	15	2	6	76	982
0.314	13	2	5	80	955
0.126	16	4	9	71	526
0.114	8	4	14	73	665
0.088	25	8	12	53	210
0.062	33	13	14	40	164
0.014	24	57	10	8	117

[a] Massic ratio expressed from analysis data. 1, CH_2O; 2, $HCOOCH_3$; 3, $(CH_3O)_2CH_2$; 4, $(CH_3)_2O$. Selectivities for carbon oxides are always less than 2%.

ties of series 2 samples are more than three times higher than those of the $SiMo_{12}H/SiO_2$ series. We have suggested by IR and Raman spectroscopy (*1*) that the Keggin unit $SiMo_{12}$ is preserved in the latter catalysts for coverages above 7 wt% Mo; at lower contents, only high-frequency bands of $SiMo_{12}$ are observed. The much higher activity for series 2 catalysts at loadings less than 10% indicates that the surfaces are not really the same in both cases. If $SiMo_{12}H$ is present on both surfaces, another species is required to account for the enhanced acidic activity.

Let us consider again the trimolybdic model on the silica surface. As reported above, the Mo-oxo species in this assumption is highly acidic: there are more acidic protons available for the reaction than in the case of well-dispersed silica-supported $SiMo_{12}H$, where the protons are trapped through interactions between the OH surface groups and the Keggin units. The presence of trimolybdic groups on the silica surface could consequently explain the enhanced activity with respect to $SiMo_{12}H/SiO_2$ catalysts.

As pointed out above, the bands likely assigned to $SiMo_{12}H$ in the Raman spectra of III-500-W and IV-500-W only appear after 2-day water exposure. *However, the samples are already active after water exposure overnight, and the catalytic activity does not significantly vary with the water exposure duration.* In other words, $SiMo_{12}H$, which seems likely to be formed according to the Raman data, is not responsible for catalytic activity or plays only a minor role in catalytic behavior.

To account for both spectroscopic and reactivity studies, we suggest that at least trimolybdic groups, in interaction with silica via Si–O–Mo bridges, are present on the Mo/SiO_2 catalysts after water exposure. Moreover, this hypothesis does not exclude the simultaneous presence on the surface of other species contributing to different extents to the catalytic activity. The characterization techniques do not allow a quantitative analysis of the species, and, moreover, each of them can emphasize just the type of

species to which it is more sensitive. *The true picture of the surface is that it is perhaps constituted of trimolybdic groups randomly connected together and to the silica and of small quantities of Keggin units, emphazised in some cases thanks to Raman spectrometry, but playing only a minor role in the catalytic reaction.* In addition, for loadings higher than 10 wt%, an important part of the molybdenum is found as "free" MoO_3, easily characterized by IR and Raman. This explains the decrease in the total activity, since crystallized MoO_3 is rather inactive (*22*).

CONCLUSION

The results discussed in this paper clearly evidence the effect of water on the properties of Mo/SiO_2 catalysts prepared from hexamolybdate.

The calcined catalysts handled in air without special exposure to water essentially exhibit redox catalytic properties toward methanol conversion. The activity of the catalysts increases when the Mo content is decreased.

The water-exposed catalysts present predominant acidic catalytic properties whatever the Mo content, showing that the acidic protons are easily available for methanol dehydration. According to IR spectra and to catalytic measurements, compared with those obtained with $SiMo_{12}H/SiO_2$ catalysts, at least fragments of Keggin units, namely trimolybdic groups, in interaction with silica via Si–O–Mo bridges, are present on the surface and are responsible for catalytic activity. This can be understood when the amphoteric character of MoO_3, which can strongly interact with water, is considered. Silica support is required to favor water adsorption and seems to act as a synergetic partner. In addition, the existence of trimolybdic groups does not exclude the simultaneous presence of $SiMo_{12}H$.

We have pointed out the possibilities and the limits of different characterization techniques. It is worth noting the importance of catalytic measurements, which offer useful additional information about the surface state.

The two series of Mo/SiO_2 catalysts studied in this paper allow us to perform either redox or acidic catalytic reactions, according to the water content. Further investigations are in progress to refine the picture of the oxo-Mo species responsible for catalytic activity and to estimate the sensitivity of the reaction to initial conditions.

ACKNOWLEDGMENTS

This work was supported by CNRS and AFME (ATP No. 2261, Catalyse hétérogène, chimie du solide et chimie de coordination). The authors thank Dr. A. Regis (Laboratory LASIR, CNRS, Thiais, France) for providing facilities to record far-infrared spectra with the Bruker 113 V FTIR spectrometer.

REFERENCES

1. (*a*) Tatibouët, J. M., Che, M., Amirouche, M., Fournier, M., and Rocchiccioli-Deltcheff, C., *J. Chem. Soc. Chem. Commun.*, 1260 (1988); (*b*) in preparation.
2. Dufaux, M., Che, M., and Naccache, C., *J. Chim. Phys.* **67,** 527 (1970).
3. Castellan, A., Bart, J. C. J., Vaghi, A., and Giordano, N., *J. Catal.* **42,** 162 (1976).
4. (*a*) Marcinkowska, K., Rodrigo, L., Kaliaguine, S., and Roberge, P. C., *J. Molec. Catal.* **33,** 189 (1985); (*b*) Stencel, J. M., Makovsky, L. E., Sarkus, T. A., De Vries, J., Thomas, R., and Moulijn, J. A., *J. Catal.* **90,** 314 (1984); (*c*) Stencel, J. M., Diehl, J. R., D'Este, J. R., Makovsky, L. E., Rodrigo, L., Marcinkowska, K., Adnot, A., Roberge, P. C., and Kaliaguine, S., *J. Phys. Chem.* **90,** 4739 (1986).
5. Payen, E., Grimblot, J., and Kasztelan, S., *J. Phys. Chem.* **91,** 6642 (1987).
6. (*a*) Cheng, C. P., and Schrader, G. L., *J. Catal.* **60,** 276 (1979); (*b*) Cheng, C. P., Ludowise, J. D., and Schrader, G. L., *Appl. Spectrosc.* **34,** 146 (1980).
7. Seyedmonir, S. R., Abdo, S., and Howe, R. F., *J. Phys. Chem.* **86,** 1233 (1982).
8. (*a*) Gajardo, P., Grange, P., and Delmon, B., *J. Phys. Chem.* **83,** 1771 (1979); (*b*) Gajardo, P., Pirotte, D., Grange, P., and Delmon, B., *J. Phys. Chem.* **83,** 1780 (1979); (*c*) Jeziorowski, H., Knözinger, H., Grange, P., and Gajardo, P., *J. Phys. Chem.* **84,** 1825 (1980).
9. Goncharova, O. I., Davydov, A. A., Yurieva, T. M., and Khokhireva, T. Kh., *Kinet. Katal.* **24,** 683 (1983).
10. Barbaux, Y., Elamrani, A. R., Payen, E., Gengem-

bre, L., Bonnelle, J. P., and Grzybowska, B., *Appl. Catal.* **44,** 117 (1988).
11. Rodrigo, L., Marcinkowska, K., Adnot, A., Roberge, P. C., Kaliaguine, S., Stencel, J. M., Makovsky, L. E., and Diehl, J. R., *J. Phys. Chem.* **90,** 2690 (1986).
12. Cornac, M., Janin, A., and Lavalley, J. C., *Infrared Phys.* **24,** 143 (1984); *Polyhedron* **5,** 183 (1986).
13. Medema, J., Van Stam, C., De Beer, V. H. J., Konings, A. J. A., and Koningsberger, D. C., *J. Catal.* **53,** 386 (1978).
14. Ono, T., Anpo, M., and Kubokawa, Y., *J. Phys. Chem.* **90,** 4780 (1986).
15. Kasztelan, S., Payen, E., and Moffat, J. B., *J. Catal.* **112,** 320 (1988).
16. (*a*) Louis, C., Tatibouët, J. M., and Che, M., *J. Catal.* **109,** 354 (1988); (*b*) Che, M., Louis, C., and Tatibouët, J. M., *Polyhedron* **5,** 123 (1986).
17. Che, M., Fournier, M., and Launay, J. P., *J. Chem. Phys.* **71,** 1954 (1979).
18. Rocchiccioli-Deltcheff, C., Thouvenot, R., and Fouassier, M., *Inorg. Chem.* **21,** 30 (1982).
19. (*a*) Andersson, G., and Magnéli, A., *Acta Chem. Scand.* **4,** 793 (1950); (*b*) Westman, S., and Magnéli, a., *Acta Chem. Scand.* **11,** 1587 (1957); (*c*) Kihlborg, L., *Ark. Kemi* **21,** 357 (1963).
20. (*a*) Lindqvist, I., *Acta Chem. Scand.* **4,** 650 (1950); **10,** 1362 (1956); (*b*) Krebs, B., *Chem. Comm.*, 50 (1970); *Acta Crystallogr. B* **28,** 2222 (1972); (*c*) Asbrink, S., and Brandt, G., *Chem. Scripta* **1,** 169 (1971).
21. This species could be constituted of layers of associated MoO_6 octahedra, connected through H_2O molecules, in a way similar to that observed in dihydrated MoO_3 (*20*).
22. Tatibouët, J. M., and Germain, J. E., *J. Catal.* **72,** 375 (1980).
23. Rocchiccioli-Deltcheff, C., Amirouche, M., Hervé, G., Fournier, M., Che, M., and Tatibouët, J. M., submitted for publication.
24. Rocchiccioli-Deltcheff, C., Fournier, M., Franck, R., and Thouvenot, R., *Inorg. Chem.* **22,** 207 (1983).
25. Fournier, M., Louis, C., Che, M., Chaquin, P., and Masure, D., *J. Catal.* **119,** 400 (1989).
26. Thouvenot, R., Fournier, M., Franck, R., and Rocchiccioli-Deltcheff, C., *Inorg. Chem.* **23,** 598 (1984).